Stationary equilibrium singularity distributions in the plane

IOP PUBLISHING NONLINEARITY

Nonlinearity **25** (2012) 495–511 doi:10.1088/0951-7715/25/2/495

Stationary equilibrium singularity distributions in the plane

P K Newton and V Ostrovskyi

Department of Aerospace and Mechanical Engineering and Department of Mathematics, University of Southern California, Los Angeles, CA 90089-1191, USA

E-mail: newton@usc.edu

Received 2 August 2011, in final form 9 December 2011
Published 20 January 2012
Online at stacks.iop.org/Non/25/495

Recommended by A L Bertozzi

Abstract

We characterize all *stationary* equilibrium point singularity distributions in the plane of logarithmic type, allowing for real, imaginary or complex singularity strengths. The dynamical system follows from the assumption that each of the N singularities moves according to the flow field generated by all the others at that point. For strength vector $\vec{\Gamma} \in \mathbb{R}^N$, the dynamical system is the classical point vortex system obtained from a singular discrete representation of the vorticity field from ideal, incompressible fluid flow. When $\vec{\Gamma} \in \Im$, it corresponds to a system of sources and sinks, whereas when $\vec{\Gamma} \in \mathbb{C}^N$ the system consists of spiral sources and sinks discussed in Kochin *et al* (1964 *Theoretical Hydromechanics* 1 (London: Interscience)). We formulate the equilibrium problem as one in linear algebra, $A\vec{\Gamma} = 0$, $A \in \mathbb{C}^{N\times N}$, $\vec{\Gamma} \in \mathbb{C}^N$, where A is a $N \times N$ complex skew-symmetric configuration matrix which encodes the geometry of the system of interacting singularities. For an equilibrium to exist, A must have a kernel and $\vec{\Gamma}$ must be an element of the nullspace of A. We prove that when N is odd, A always has a kernel, hence there is a choice of $\vec{\Gamma}$ for which the system is a stationary equilibrium. When N is even, there may or may not be a non-trivial nullspace of A, depending on the relative position of the points in the plane. We provide examples of evenly and randomly distributed points on curves such as circles, figure eights, flower-petal configurations and spirals. We then show how to classify the stationary equilibria in terms of the singular spectrum of A.

Mathematics Subject Classification: 34A34, 34C60, 35Q35, 37N10

PACS numbers: 05.45.−a; 47.32.C−

1. Introduction

Consider the vector field at $z = 0$ governed by the complex dynamical system:

$$\dot{z}^* = \frac{\Gamma}{2\pi \mathrm{i}} \frac{1}{z}, \qquad z(t) \in \mathbb{C}, \quad \Gamma \in \mathbb{C}, \quad t \in \mathbb{R} > 0, \tag{1}$$

where z^* denotes the complex conjugate of $z(t)$. Letting $z(t) = r(t)\exp(\mathrm{i}\theta(t))$, $\Gamma = \Gamma_r + i\Gamma_i$, gives

$$\dot{r} = \frac{\Gamma_i}{2\pi r}, \tag{2}$$

$$\dot{\theta} = \frac{\Gamma_r}{2\pi r^2}, \tag{3}$$

from which it is easy to see that

$$r(t) = \sqrt{\left(\frac{\Gamma_i}{2\pi}\right) t + r^2(0)}, \tag{4}$$

$$\theta(t) = \begin{cases} \left(\dfrac{\Gamma_r}{\Gamma_i}\right) \ln\left(\left(\dfrac{\Gamma_r}{\Gamma_i}\right) t + r^2(0)\right) & \text{if } \Gamma_i \neq 0 \\ \dfrac{\Gamma_r t}{2\pi r^2(0)} + \theta(0) & \text{if } \Gamma_i = 0. \end{cases} \tag{5}$$

When $\Gamma_r \neq 0$, $\Gamma_i = 0$, the field is that of a classical point vortex (figures 1(*a*) and (*b*)); when $\Gamma_r = 0$, $\Gamma_i \neq 0$ it is a source ($\Gamma_i > 0$) or sink ($\Gamma_i < 0$) (figures 1(*c*) and (*d*)), while when $\Gamma_r \neq 0$, $\Gamma_i \neq 0$, it is a spiral-source or sink (figures 1(*e*) and (*h*).

A collection of N of these point singularities, each located at $z = z_\beta(t)$, $\beta = 1, \ldots, N$, by linear superposition, produces the field:

$$\dot{z}^* = \frac{1}{2\pi \mathrm{i}} \sum_{\beta=1}^{N} \frac{\Gamma_\beta}{z - z_\beta}; \qquad z(t) \equiv x(t) + \mathrm{i}y(t) \in \mathbb{C}, \quad \Gamma_\beta \in \mathbb{C}. \tag{6}$$

Then, if we advect each by the velocity field generated by all the others[1], we arrive at the complex dynamical system:

$$\dot{z}^*_\alpha = \frac{1}{2\pi \mathrm{i}} \sum_{\beta=1}^{{}'N} \frac{\Gamma_\beta}{z_\alpha - z_\beta}; \qquad z_\alpha(t) \equiv x_\alpha(t) + \mathrm{i}y_\alpha(t) \in \mathbb{C}, \quad \Gamma_\beta \in \mathbb{C}, \tag{7}$$

where $'$ indicates that $\beta \neq \alpha$. In this paper we characterize all *stationary* equilibria of (7), namely solutions for which $\dot{z}^*_\alpha(t) = 0$. For this, we have the N coupled equations:

$$\sum_{\beta=1}^{{}'N} \frac{\Gamma_\beta}{z_\alpha - z_\beta} = 0, \qquad (\alpha = 1, \ldots, N), \tag{8}$$

where we are interested in positions z_α and strengths Γ_α for which this nonlinear algebraic system is satisfied. Since equation (8) is *linear* in the Γ, it can more productively be written in matrix form

$$A\vec{\Gamma} = 0 \tag{9}$$

where $A \in \mathbb{C}^{N\times N}$ is evidently a skew-symmetric matrix $A = -A^T$, with entries $[a_{\alpha\alpha}] = 0$, $[a_{\alpha\beta}] = \frac{1}{z_\alpha - z_\beta} = -[a_{\beta\alpha}]$. We call A the *configuration matrix* associated with the interacting

[1] One might characterize this dynamical assumption by saying that each singularity 'goes with the flow'.

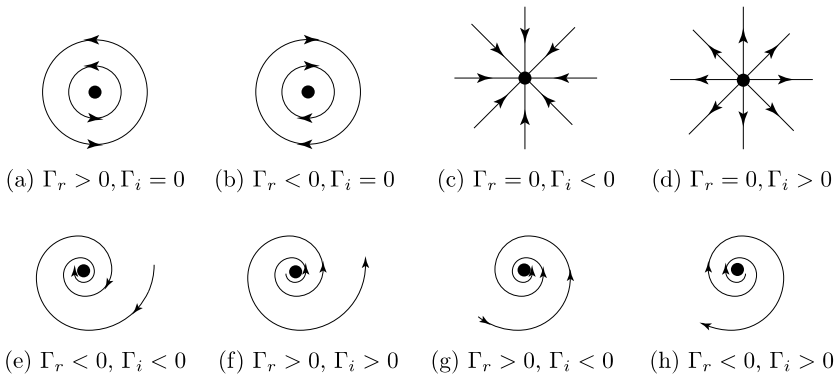

(a) $\Gamma_r > 0, \Gamma_i = 0$ (b) $\Gamma_r < 0, \Gamma_i = 0$ (c) $\Gamma_r = 0, \Gamma_i < 0$ (d) $\Gamma_r = 0, \Gamma_i > 0$

(e) $\Gamma_r < 0, \Gamma_i < 0$ (f) $\Gamma_r > 0, \Gamma_i > 0$ (g) $\Gamma_r > 0, \Gamma_i < 0$ (h) $\Gamma_r < 0, \Gamma_i > 0$

Figure 1. All possible flowfields at the singular point $z = 0$ associated with the dynamical system (1).

particle system (7). The collection of points $\{z_1(0), z_2(0), \ldots, z_N(0)\}$ in the complex plane is called the *configuration*. From (9), we can conclude that the points z_α are in a stationary equilibrium configuration if $\det(A) = 0$, i.e. there is at least one zero eigenvalue of A. If the corresponding eigenvector is real, the configuration is made up of point vortices. If it is imaginary, it is made up of sources and sinks. If it is complex, it is made up of spiral sources and sinks. Note also that if $\frac{\mathrm{d}z_\alpha^*}{\mathrm{d}t} = 0$, then one can prove that $\frac{\mathrm{d}^n z_\alpha^*}{\mathrm{d}t^n} = 0$ for any n. It follows that:

Proposition 1. *For a given configuration of N points $\{z_1, z_2, \ldots, z_N\}$ in the complex plane, there exists a set of singularity strengths $\vec{\Gamma}$ for which the configuration is a stationary equilibrium solution of the dynamical system (7) iff A has a kernel, or equivalently, if there is at least one zero eigenvalue of A. If the nullspace dimension of A is one, i.e. there is only one zero eigenvalue, the choice of $\vec{\Gamma}$ is unique (up to a multiplicative constant). If the nullspace dimension is greater than one, the choice of $\vec{\Gamma}$ is not unique and can be any linear combination of the basis elements of null(A).*

The equilibria we consider in this paper all have one-dimensional nullspaces and odd N. The more delicate cases of equilibria with higher dimensional nullspaces and even N are deferred to a separate study.

We mention here work of Campbell and Kadtke (1987) and Kadtke and Campbell (1987) in which a different technique is described to find stationary solutions to (7), and O'Neil's work (1987) based on his PhD thesis. Others have considered various dynamical questions associated with different types of singularities in the plane (other than the large literature on point-vortex singularities), mostly using the 'fluid dynamics' assumption that the singularities go with the flow. In this context, works of Novikov and Sedov (1983), Novikov and Novikov (1996), Novikov (2003), Yanovsky *et al* (2009), Tur *et al* (2011) and Llewellyn Smith (2011) are most relevant and interesting. We point out, however, that other dynamical assumptions could be used and would lead to different dynamical systems.

2. General properties of the configuration matrix

Since A is skew-symmetric, it follows that

$$\det(A) = \det(-A^T) = (-1)^N \det(A^T) = \det(A^T). \tag{10}$$

Hence, for N *odd*, we have $-\det(A^T) = \det(A^T)$, which implies $\det(A^T) = 0$.

Proposition 2. *When N is odd, A always has at least one zero eigenvalue, hence for any configuration there exists a choice $\vec{\Gamma} \in \mathbb{C}$ for which the system is a stationary equilibrium.*

When N is even, there may or may not be a stationary equilibrium, depending on whether or not A has a non-trivial nullspace. In general, we would like to determine a basis set for the nullspace of A for a given configuration, i.e. the set of all strengths for which a given configuration remains fixed. Other important general properties of skew-symmetric matrices are listed below:

(i) The eigenvalues always come in pairs $\pm\lambda$. If N is odd, there is one unpaired eigenvalue that is zero.
(ii) If N is even, $\det(A) = Pf(A)^2 \geqslant 0$, where Pf is the Pfaffian.
(iii) Real skew-symmetric matrices have pure imaginary eigenvalues.

Recall that every matrix can be written as the sum of a Hermitian matrix ($B = B^\dagger$) and a skew-Hermitian matrix ($C = -C^\dagger$). To see this, note

$$A \equiv \tfrac{1}{2}(A + A^\dagger) + \tfrac{1}{2}(A - A^\dagger). \tag{11}$$

Here, $B \equiv \frac{1}{2}(A + A^\dagger) = B^\dagger$ and $C \equiv \frac{1}{2}(A - A^\dagger) = -C^\dagger$. A matrix is *normal* if $AA^\dagger = A^\dagger A$, otherwise it is *non-normal*. If we calculate $AA^\dagger - A^\dagger A$, where $A = B + C$ as above, then it is easy to see that

$$AA^\dagger - A^\dagger A = 2(CB - BC). \tag{12}$$

Therefore, if $B = 0$ or $C = 0$, A is normal.

Proposition 3. *All Hermitian or skew-Hermitian matrices are normal.*

The generic configuration matrix A arising from (9) is, however, non-normal.

2.1. Spectral decomposition of normal and non-normal matrices

For normal matrices, the following spectral decomposition holds.

Proposition 4. *A is a normal matrix $\Leftrightarrow$ A is unitarily diagonalizable, i.e.*

$$A = Q\Lambda Q^\dagger \tag{13}$$

where Q is unitary.

Here, the columns of Q are the N linearly independent eigenvectors of A that can be made mutually orthogonal. The matrix Λ is a diagonal matrix with the N eigenvalues down the diagonal. See Golub and Van Loan (1996) for details.

In general, however, for the system of interacting particles governed by (8), (9), $A \in \mathbb{C}^{N\times N}$ will be a non-normal matrix. The most comprehensive decomposition of A in this case is the singular value decomposition (Golub and Van Loan (1996), Trefethen and Bau (1997)). It is a factorization that greatly generalizes the spectral decomposition of a normal matrix, and it is available for any matrix.

The N singular values, $\sigma^{(i)}$ $(i = 1, \ldots, N)$, of A, are non-negative real numbers that satisfy

$$A\boldsymbol{v}^{(i)} = \sigma^{(i)}\boldsymbol{u}^{(i)}; \qquad A^\dagger\boldsymbol{u}^{(i)} = \sigma^{(i)}\boldsymbol{v}^{(i)}, \tag{14}$$

where $\boldsymbol{u}^{(i)} \in \mathbb{C}^N$ and $\boldsymbol{v}^{(i)} \in \mathbb{C}^N$. The vector $\boldsymbol{u}^{(i)}$ is called the left-singular vector associated with $\sigma^{(i)}$, while $\boldsymbol{v}^{(i)}$ is the right-singular vector. In terms of these, the matrix A has the factorizations

$$A = U\Sigma V^\dagger = \sum_{i=1}^{k} \sigma^{(i)} \boldsymbol{u}^{(i)} \boldsymbol{v}^{(i)T}, \qquad (k \leqslant N) \tag{15}$$

where $U \in \mathbb{C}^{N\times N}$ in unitary, $V \in \mathbb{C}^{N\times N}$ is unitary, and $\Sigma \in \mathbb{R}^{N\times N}$ is diagonal. (15) is the non-normal analogue of the spectral decomposition formula (13) where the summation term on the right-hand side gives an (optimal) representation of A as a linear combination of rank-one matrices with weightings governed by the singular values ordered from largest to smallest. Here, the rank of A is k. The columns of U are the left-singular vectors $\boldsymbol{u}^{(i)}$, while the columns of V are the right-singular vectors $\boldsymbol{v}^{(i)}$. The matrix Σ is given by

$$\Sigma = \begin{pmatrix} \sigma^{(1)} & \cdots & 0 \\ & \ddots & \\ 0 & \cdots & \sigma^{(N)} \end{pmatrix} \in \mathbb{R}^{N\times N}. \tag{16}$$

The singular values can be ordered so that $\sigma^{(1)} \geqslant \sigma^{(2)} \geqslant \ldots \geqslant \sigma^{(N)} \geqslant 0$ and one or more may be zero. As is evident from multiplying the first equation in (14) by $A^\dagger$ and the second by A,

$$(A^\dagger A - \sigma^{(i)2})\boldsymbol{v}^{(i)} = 0; \qquad (AA^\dagger - \sigma^{(i)2})\boldsymbol{u}^{(i)} = 0, \tag{17}$$

the singular values squared are the eigenvalues of the *covariance* matrices $A^\dagger A$ or $AA^\dagger$, which have the same eigenvalue structure, while the left-singular vectors $\boldsymbol{u}^{(i)}$ are the eigenvectors of $AA^\dagger$, and the right-singular vectors $\boldsymbol{v}^{(i)}$ are the eigenvectors of $A^\dagger A$. From (14), we also note that the right-singular vectors $\boldsymbol{v}^{(i)}$ corresponding to $\sigma^{(i)} = 0$ form a basis for the nullspace of A. Because of (9), we seek configuration matrices with one or more singular values that are zero.

3. Collinear equilibria

For the special case in which all the particles lie on a straight line, there is no loss in assuming $z_\alpha = x_\alpha \in \mathbb{R}$. Then $A \in \mathbb{R}^{N\times N}$, A is a normal skew-symmetric matrix, and the eigenvalues are pure imaginary. As an example, consider the collinear case $N = 3$. Let the particle positions be $x_1 < x_2 < x_3$, with corresponding strengths $\Gamma_1, \Gamma_2, \Gamma_3$. The A matrix is then given by

$$A = \begin{bmatrix} 0 & \dfrac{1}{x_1 - x_2} & \dfrac{1}{x_1 - x_3} \\ \dfrac{1}{x_2 - x_1} & 0 & \dfrac{1}{x_2 - x_3} \\ \dfrac{1}{x_3 - x_1} & \dfrac{1}{x_3 - x_2} & 0 \end{bmatrix}. \tag{18}$$

Since N is odd, we have $\det(A) = 0$. The other two eigenvalues are given by

$$\lambda_{123} = \pm \mathrm{i} \sqrt{\frac{1}{(x_2 - x_1)^2} + \frac{1}{(x_3 - x_2)^2} + \frac{1}{(x_3 - x_1)^2}}, \tag{19}$$

which is invariant under cyclic permutations of the indices ($\lambda_{123} = \lambda_{231} = \lambda_{312}$). We can scale the length of the configuration so that the distance between x_1 and x_3 is one, hence without

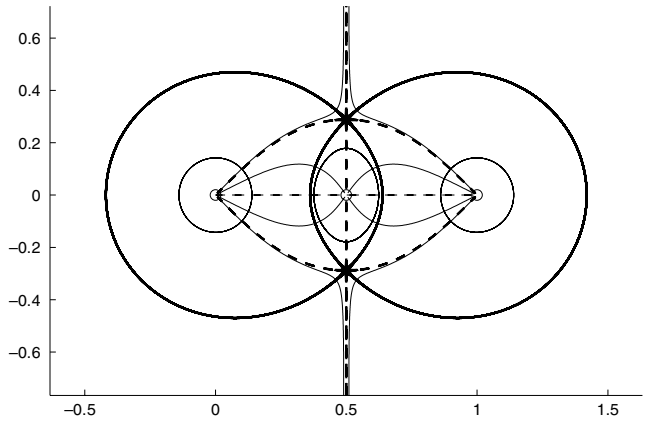

Figure 2. $N = 3$ evenly distributed point vortices on a line with strengths $\Gamma_1 = 1, \Gamma_2 = -\frac{1}{2}$, $\Gamma_3 = 1$, in equilibrium. The far field is that of a point vortex at the centre of vorticity of the system. Solid streamline pattern is for point vortices, dashed streamline pattern is for source/sink system. The patterns are orthogonal.

loss of generality, let $x_1 = 0, x_2 = x, x_3 = 1$. The other two eigenvalues are then given by the formula

$$\lambda = \pm \mathrm{i} \sqrt{\frac{(1 - x + x^2)^2}{x^2(1-x)^2}}. \tag{20}$$

It is easy to see that the numerator has no roots in the interval $(0, 1)$, hence the nullspace dimension of A is one. The nullspace vector is then given (uniquely up to multiplicative constant) by

$$\vec{\Gamma} = \begin{bmatrix} 1 \\ -\left(\dfrac{x_3 - x_2}{x_3 - x_1}\right) \\ \left(\dfrac{x_3 - x_2}{x_2 - x_1}\right) \end{bmatrix}. \tag{21}$$

For the special symmetric case $x_3 - x_1 = 1$, $x_3 - x_2 = 1/2$, $x_2 - x_1 = 1/2$, we have $\Gamma_1 = 1, \Gamma_2 = -1/2, \Gamma_3 = 1$. We show this case in figure 2 along with the separatrices associated with the corresponding flowfield generated by the singularities. Since the sum of the strengths of the three vortices is $\Gamma_1 + \Gamma_2 + \Gamma_3 = 1 - 1/2 + 1 = 3/2$, the far field is that of a point vortex of strength $\Gamma = 3/2$. Interestingly, for the collinear cases, since A is real, the nullspace vector is either real, or if multiplied by i, is pure imaginary. Hence, each collinear configuration of point vortices obtained with a given $\vec{\Gamma} \in \mathbb{R}$ is also a collinear configuration of sources/sinks with corresponding strengths given by $\mathrm{i}\vec{\Gamma}$. The corresponding streamline pattern for the source/sink configuration, as shown in the dashed curves of figure 2, is the orthogonal complement of the curves corresponding to the point-vortex case.

For N even, we cannot say *a priori* whether or not $\det(A) = 0$ as the case for $N = 2$ shows. For this, the A matrix is

$$A = \begin{bmatrix} 0 & \dfrac{1}{x_1 - x_2} \\ \dfrac{1}{x_2 - x_1} & 0 \end{bmatrix} = \begin{bmatrix} 0 & \dfrac{1}{d} \\ -\dfrac{1}{d} & 0 \end{bmatrix}. \tag{22}$$

The eigenvalues are $\lambda = \pm \mathrm{i}/d$, hence there is no equilibrium (except in the limit $d \to \infty$).

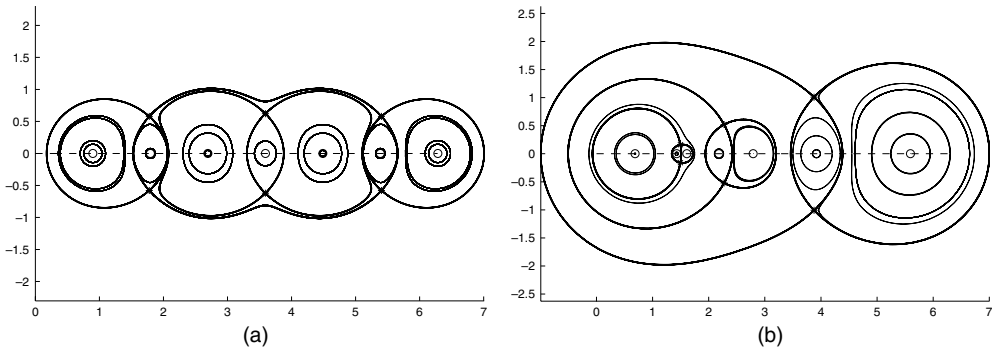

Figure 3. (*a*) $N = 7$ evenly distributed point vortices on a line. The far field is that of a point vortex at the centre of vorticity of the system. Because of the symmetry of the spacing, the vortex strengths are symmetric about the central point x_4 which also corresponds to the centre of vorticity. (*b*) $N = 7$ randomly distributed point vortices on a line. The far field is that of a point vortex at the centre of vorticity of the system.

We show in figures 3(*a*) and (*b*) two representative examples of collinear stationary point-vortex equilibria for $N = 7$, along with their corresponding global streamline patterns. In figure 3(*a*) we deposit seven evenly spaced points on a line and solve for the nullspace vector to obtain the singularity strengths (ordered from left to right)

$$\vec{\Gamma} = (1.0000, -0.5536, 0.9212, -0.5797, 0.9212, -0.5536, 1.0000), \tag{23}$$

$$\sum_{\alpha} \Gamma_\alpha = 2.1555. \tag{24}$$

Because of the even spacing, the strengths are symmetric about the central point x_4 ($\Gamma_1 = \Gamma_7, \Gamma_2 = \Gamma_6, \Gamma_3 = \Gamma_5$), which is also the location of the centre of vorticity $\sum_{\alpha=1}^{7} \Gamma_\alpha x_\alpha$. Figure 3(*b*) shows a fixed equilibrium corresponding to seven points randomly placed on a line. The nullspace vector for this case is (ordered from left to right)

$$\vec{\Gamma} = (1.0000, -0.5071, 0.5342, -0.4007, 0.2815, -0.2505, 1.0743), \tag{25}$$

$$\sum_{\alpha} \Gamma_\alpha = 1.7317. \tag{26}$$

In both cases, the singularities are all point vortices (or source/sink systems) hence are examples of collinear equilibria such as those discussed in Aref (2007a, 2007b, 2009) and Aref *et al* (2003) where the strengths are typically chosen as equal. The streamline pattern at infinity in both cases is that of a single point vortex of strength $\sum_{\alpha=1}^{7} \Gamma_\alpha \neq 0$ located at the centre of vorticity $\sum_{\alpha=1}^{7} \Gamma_\alpha x_\alpha$.

4. Triangular equilibria

The case $N = 3$ is somewhat special and worth treating separately. Given any three points $\{z_1, z_2, z_3\}$ in the complex plane, the corresponding configuration matrix A is

$$A = \begin{bmatrix} 0 & \dfrac{1}{z_1 - z_2} & \dfrac{1}{z_1 - z_3} \\ \dfrac{1}{z_2 - z_1} & 0 & \dfrac{1}{z_2 - z_3} \\ \dfrac{1}{z_3 - z_1} & \dfrac{1}{z_3 - z_2} & 0 \end{bmatrix}. \tag{27}$$

There is no loss of generality in choosing two of the points along the real axis, one at the origin of our coordinate system, the other at $x = 1$. Hence we set $z_1 = 0$, $z_2 = 1$, and we let $z_3 \equiv z$. Then A is written much more simply:

$$A = \begin{bmatrix} 0 & -1 & -\dfrac{1}{z} \\ 1 & 0 & \dfrac{1}{1-z} \\ \dfrac{1}{z} & \dfrac{1}{z-1} & 0 \end{bmatrix}. \tag{28}$$

Since N is odd, one of the eigenvalues of A is zero. The other two are given by

$$\lambda = \pm \mathrm{i}\sqrt{\frac{1}{z^2} + \frac{1}{(1-z)^2} + 1} = \pm \mathrm{i}\sqrt{\frac{(1-z+z^2)^2}{z^2(1-z)^2}}. \tag{29}$$

When the numerator is not zero, the nullspace dimension is one and it is easy to see that the nullspace of A is given by

$$\vec{\Gamma} = \begin{bmatrix} \dfrac{1}{z-1} \\ -\dfrac{1}{z} \\ 1 \end{bmatrix}. \tag{30}$$

However, the numerator is zero at the points:

$$z = \exp\left(\frac{\pi \mathrm{i}}{3}\right), \exp\left(\frac{5\pi \mathrm{i}}{3}\right), \tag{31}$$

at which $\Re z = \frac{1}{2}$, $\Im z = \pm\frac{\sqrt{3}}{2}$. This forms an equilateral triangle in which case the nullspace dimension is three. We have thus proven the following.

Proposition 5. *For three point vortices, or for three sources/sinks, the only stationary equilibria are collinear. In this case, the nullspace dimension of A is one and is given by (30). For the equilateral triangle configuration, the nullspace dimension is three.*

We show a fixed equilibrium equilateral triangle state in figure 4(*a*) along with the corresponding streamline pattern. Figures 4(*b*), (*c*) and (*d*) show examples of $N = 3$ triangular states that are not equilateral.

5. Equilibria along prescribed curves

We now ask a more general and interesting question. Given any curve in the complex plane, if we distribute points $\{z_\alpha\}$, $(\alpha = 1, \ldots, N)$ along the curve, is it possible to find a strength vector $\vec{\Gamma}$ so that the configuration is stationary? The answer is yes, if N is odd, and sometimes, if N is even.

Figures 5–9 show a collection of stationary equilibria along curves that we prescribe. First, figure 5 shows 7 points placed randomly in the plane, with the singularity strengths obtained from the nullspace of A so that the system is in equilibrium. The strengths are given by $\vec{\Gamma} = (1.0000, -0.7958 + 1.0089\mathrm{i}, -1.3563 - 0.4012\mathrm{i}, 0.0297 + 0.1594\mathrm{i}, 0.9155 + 0.3458\mathrm{i}, -2.0504 - 0.8776\mathrm{i}, -0.1935 - 1.0802\mathrm{i})^T$ with the sum given by $-2.4508 - 0.8449\mathrm{i}$. Thus, the far field is that of a spiral-sink configuration. Figure 6(*a*) shows the case of $N = 7$ points distributed evenly around a circle. The nullspace vector is given by $\vec{\Gamma} = (1.0000, -0.9010 + 0.4339\mathrm{i}, 0.6235 - 0.7818\mathrm{i}, -0.2225 + 0.9749\mathrm{i}, -0.2225$

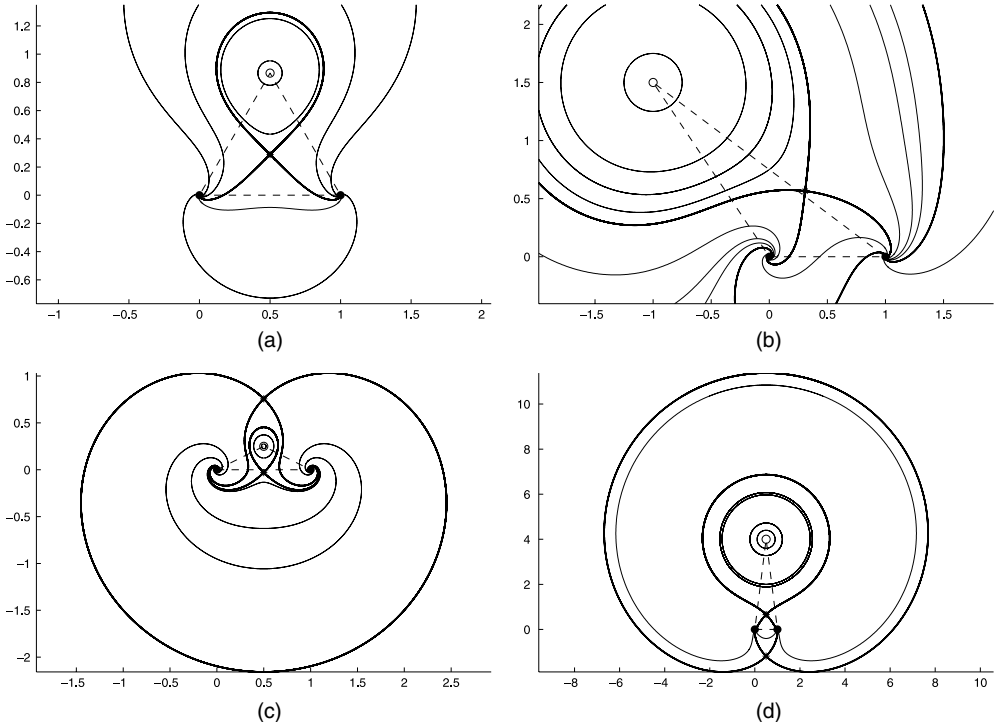

Figure 4. (*a*) $N = 3$ equilateral triangle configuration with corresponding streamline pattern. The strengths are given by $\Gamma_1 = 1.0000$, $\Gamma_2 = -0.5000 + 0.8660\mathrm{i}$, $\Gamma_3 = -0.5000 + 0.8660\mathrm{i}$. (*b*) $N = 3$ non-equilateral triangular state with corresponding streamline pattern. The strengths are given by $\Gamma_1 = 1.0000$, $\Gamma_2 = 0.3077 + 0.4615\mathrm{i}$, $\Gamma_3 = -0.3200 - 0.2400\mathrm{i}$. (*c*) $N = 3$ obtuse isosceles triangle state. The strengths are given by $\Gamma_1 = 1.0000$, $\Gamma_2 = -1.6000 + 0.8000\mathrm{i}$, $\Gamma_3 = -1.6000 - 0.8000\mathrm{i}$. (*d*) $N = 3$ acute isosceles triangle state. The strengths are given by $\Gamma_1 = 1.0000$, $\Gamma_2 = -0.0308 + 0.2462\mathrm{i}$, $\Gamma_3 = -0.0308 - 0.2462\mathrm{i}$.

$-0.9749\mathrm{i}, 0.6235 + 0.7818\mathrm{i}, -0.9010 - 0.4339\mathrm{i})^T$. For this very symmetric case, the sum of the strengths is zero, hence in a sense, the far field vanishes. Figure 6(*b*) shows the case of $N = 7$ points placed at random positions on a circle. Here, the nullspace vector is given by $\vec{\Gamma} = (1.0000, -0.6342 + 0.4086\mathrm{i}, 0.3699 - 0.5929\mathrm{i}, -0.1501 + 0.6135\mathrm{i}, -0.2483 - 0.9884\mathrm{i}, 0.2901 + 0.3056\mathrm{i}, -0.3595 - 0.2686\mathrm{i})^T$. The random placement of points breaks the symmetry of the previous case and the sum of strengths is given by $0.2649 - 0.5222\mathrm{i}$ which corresponds to a spiral-sink. In figure 7 we show equilibrium distribution of points along a curve we call a 'flower-petal', given by the formula $r(\theta) = \cos(2\theta)$, $0 \leqslant \theta \leqslant 2\pi$. In figure 7(*a*) we distribute them evenly on the curve, while in figure 7(*b*) we distribute them randomly. The particle strengths from the configuration in figure 7(*a*) are $\vec{\Gamma} = (1.0000, 0.1824 + 0.1498\mathrm{i}, -0.9892 - 0.9103\mathrm{i}, -0.1378 - 0.5333\mathrm{i}, -0.1378 + 0.5333\mathrm{i}, -0.9892 + 0.9103\mathrm{i}, 0.1824 - 0.1498\mathrm{i})^T$ with sum equaling -0.8892 corresponding to a far field point vortex. Figure 7(*b*) shows particles distributed randomly on the same flower-petal curve. Here, the particle strengths are $\vec{\Gamma} = (1.0000, 0.2094 - 0.4071\mathrm{i}, -0.3009 + 0.3003\mathrm{i}, 0.0404 - 0.2864\mathrm{i}, -0.1779 + 0.2773\mathrm{i}, 0.4236 + 0.8052\mathrm{i}, -0.4702 - 0.3304\mathrm{i})^T$, with sum given by $.7244 + .3589\mathrm{i}$. Hence the far field corresponds to a source-spiral. We note that it is interesting that the far field behaviour is determined both by the distribution of points along the curve as well as the shape of the curve for these relatively small values of N. We suspect

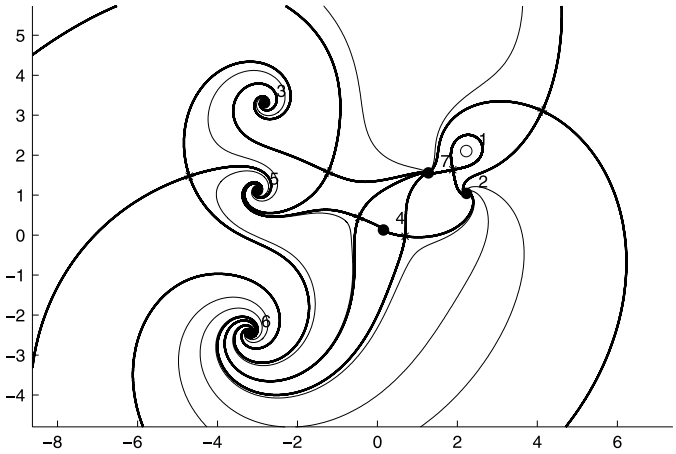

Figure 5. Stationary equilibrium for seven points placed at random locations in the plane. The far field is a spiral-sink (figure 1(*e*)) with $\sum \Gamma_\alpha = -2.4508 - 0.8449\mathrm{i}$.

that as N increases, thus filling out the curve shape more effectively, the far field behaviour will indeed be dictated more and more by the shape of the curve being filled out.

Figure 8(*a*) shows $N = 7$ points distributed evenly on a spiral curve given by $r(\theta) = \theta/6$. The particle strengths are given by $\vec{\Gamma} = (1.0000, -0.3849 + 0.3476\mathrm{i}, 0.4891 - 0.5497\mathrm{i}, 0.0621 + 0.4829\mathrm{i}, -0.1117 - 0.5650\mathrm{i}, 0.3174 + 0.1044\mathrm{i}, -0.4743 - 0.0839\mathrm{i})^T$ with sum equaling $0.8976 - 0.2636\mathrm{i}$. Figure 8(*b*) shows the points distributed randomly on the spiral curve. The particle strengths are $\vec{\Gamma} = (1.0000, -0.5784 + 0.2279\mathrm{i}, 0.9560 - 1.1986\mathrm{i}, 0.0535 + 0.1732\mathrm{i} - 0.0563 - 0.1759\mathrm{i}0.4595 + 0.0514\mathrm{i} - 0.4483 + 0.0235\mathrm{i})^T$, with sum given by $1.3861 - 0.8985\mathrm{i}$. Hence the far field in both cases corresponds to a source-spiral.

The last two configurations, shown in figures 9(*a*) and (*b*), are equilibria distributed along figure eight curves, given by the formulae $r(\theta) = \cos^2(\theta)$, $0 \leqslant \theta \leqslant 2\pi$. In figure 9(*a*) we distribute the points evenly around the curve, which gives rise to strengths $\vec{\Gamma} = (1.0000, -0.2734 + 0.5350\mathrm{i}, 0.0239 - 0.2080\mathrm{i}, 0.1063 - 0.0517\mathrm{i}, 0.1063 + 0.0517\mathrm{i}, 0.0239 + 0.2080\mathrm{i}, -0.2734 - 0.5350\mathrm{i})^T$, whose sum is 0.7136, thus a far field point vortex. In contrast, when the points are distributed randomly around the same curve, as in figure 9(*b*), the strengths are given by $\vec{\Gamma} = (1.0000, -0.1054 + 0.5724\mathrm{i}, -0.0174 - 0.4587\mathrm{i}, 0.9208 + 1.2450\mathrm{i}, -0.0460 - 0.4577\mathrm{i}, -0.5292 + 0.2371\mathrm{i}, -0.2543 - 0.0921\mathrm{i})^T$, with sum equaling $0.9685 + 1.0460\mathrm{i}$, hence a far field source-spiral. As in the flower petal example, the distribution of points along the curve changes the far field behaviour.

6. Classification of equilibria in terms of the singular spectrum

Previously, the nullspace of A was used to produce stationary equilibria along prescribed curves in the plane. Here we describe how to use the non-zero singular spectrum of A to classify the equilibria when A has a kernel, which is useful due to the fact that when one allows for general particle strengths, there exist many equilibria. Categorizing them so that quantitative comparisons can be made becomes increasingly more important as N increases. Here we introduce some important spectral diagnostics for this purpose.

Let $\sigma^{(i)}$, $\mathrm{i} = 1, \ldots, k < N$ denote the non-zero singular values of the configuration matrix A, arranged in descending order $\sigma^{(1)} \geqslant \sigma^{(2)} \geqslant \cdots \geqslant \sigma^{(k)} > 0$. First we normalize each of

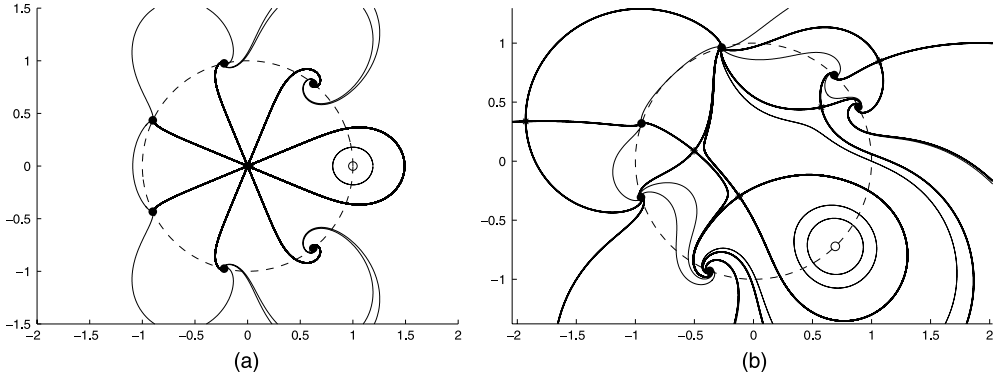

Figure 6. (*a*) $N = 7$ evenly distributed points on a circle (dashed curve) in equilibrium. Because of the symmetry of the configuration, $\sum \Gamma_\alpha = 0$, hence the far field vanishes. (*b*) $N = 7$ randomly distributed particles on a circle (dashed curve) in equilibrium along with the corresponding streamline pattern. The far field streamline pattern is that of a spiral-sink (figure 1(*g*)) since $\sum \Gamma_\alpha = 0.2649 - 0.5222\mathrm{i}$.

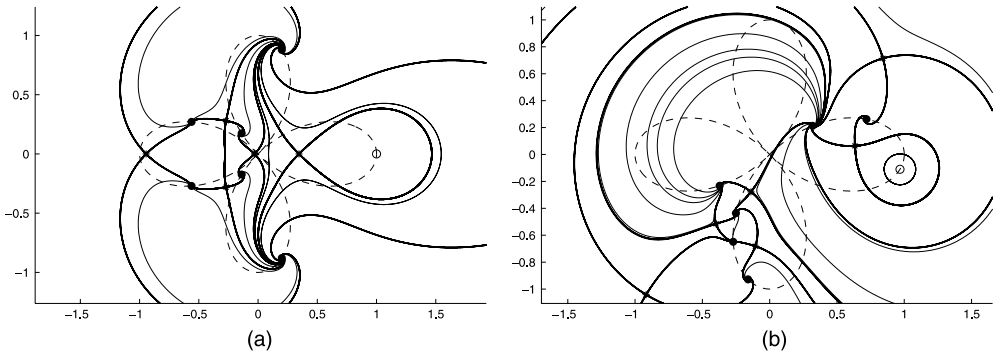

Figure 7. (*a*) $N = 7$ evenly distributed particles in equilibrium on the curve $r(\theta) = \cos(2\theta)$ (dashed curve) along with the corresponding streamline pattern. The far field corresponds to a point vortex since $\sum \Gamma_\alpha = -0.8892$. (*b*) $N = 7$ randomly distributed particles in equilibrium on the curve $r(\theta) = \cos(2\theta)$ (dashed curve). The far field corresponds to a source-spiral (figure 1(*f*)) since $\sum \Gamma_\alpha = 0.7244 + 0.3589\mathrm{i}$.

the singular values so that they sum to one:

$$\hat{\sigma}^{(i)} \equiv \sigma^{(i)} \Big/ \sum_{j=1}^{k} \sigma^{(j)}. \tag{32}$$

Then

$$\sum_{\mathrm{i}=1}^{k} \hat{\sigma}^{(i)} = 1, \tag{33}$$

and the string of k numbers arranged from largest to smallest: $(\hat{\sigma}^{(1)}, \hat{\sigma}^{(2)}, \ldots, \hat{\sigma}^{(k)})$ is the 'spectral representation' of the equilibrium which can also be thought of as a probability distribution because of the normalization. The rate at which the $\hat{\sigma}^{'(i)}s$ $(i = 1, \ldots, k)$ decay from largest to smallest is encoded in a scalar quantity called the Shannon entropy, S, of the matrix (see Shannon (1948) and more recent discussions associated with vortex lattices in

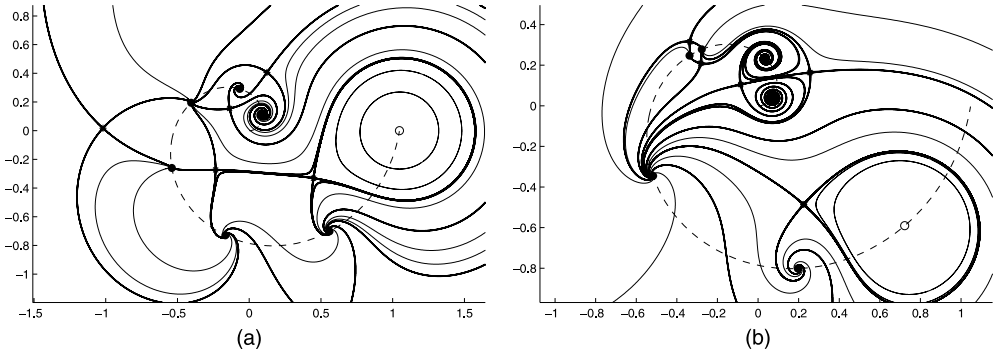

Figure 8. (*a*) $N = 7$ evenly distributed particles in equilibrium on the curve $r(\theta) = \theta/6$ (dashed curve) along with the corresponding streamline pattern. The far field corresponds to a source-spiral (figure 1(*f*)) since $\sum \Gamma_\alpha = 0.8976 - 0.2636\mathrm{i}$. (*b*) $N = 7$ randomly distributed particles in equilibrium on the curve $r(\theta) = \theta/6$ (dashed curve). The far field corresponds to a source-spiral (figure 1(*f*)) since $\sum \Gamma_\alpha = 1.3861 - 0.8985\mathrm{i}$.

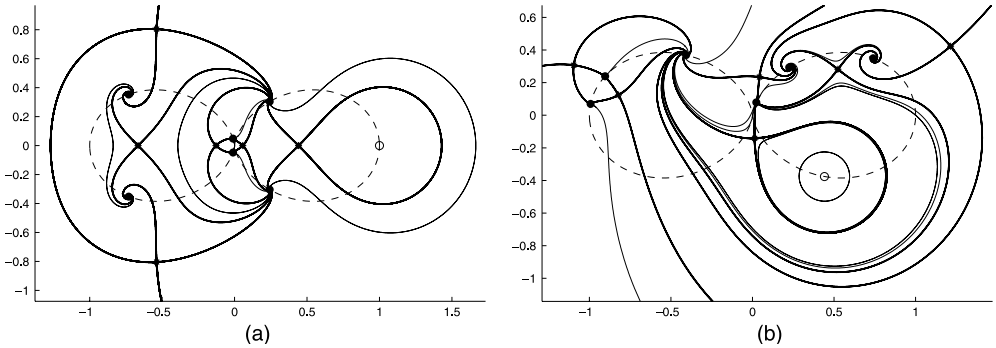

Figure 9. (*a*) $N = 7$ evenly distributed particles in equilibrium on the curve $r(\theta) = \cos^2(\theta)$ (dashed curve). The far field corresponds to a point vortex since $\sum \Gamma_\alpha = 0.7136$. (*b*) $N = 7$ randomly distributed particles in equilibrium on the curve $r(\theta) = \cos^2(\theta)$ (dashed curve). The far field corresponds to a source-spiral (figure 1(*f*)) since $\sum \Gamma_\alpha = 0.9685 + 1.0460\mathrm{i}$.

Newton and Chamoun (2009)):

$$S = -\sum_{i=1}^{k} \hat{\sigma}^{(i)} \log \hat{\sigma}^{(i)}. \tag{34}$$

With this representation, spectra that drop off rapidly from highest to lowest, are 'low-entropy equilibria' ('pure' states using the analogy of von Neumann entropy from quantum mechanics), whereas those that drop off slowly (even distribution of normalized singular values) are 'high-entropy equilibria' ('maximally mixed' states using the terminology of von Neumann entropy). Note that from the representation (15), low-entropy equilibria have configuration matrix representations that are dominated in size by a small number of terms, whereas the configuration matrices of high-entropy equilibria equilibria have terms that are more equal in size. See Newton and Chamoun (2009) for more detailed discussions in the context of relative equilibrium configurations, and the original report of Shannon (1948) which has illuminating discussions of entropy, information content, and its interpretations with respect to randomness. An entry into discussions of 'von Neumann entropy', which in some ways is more relevant

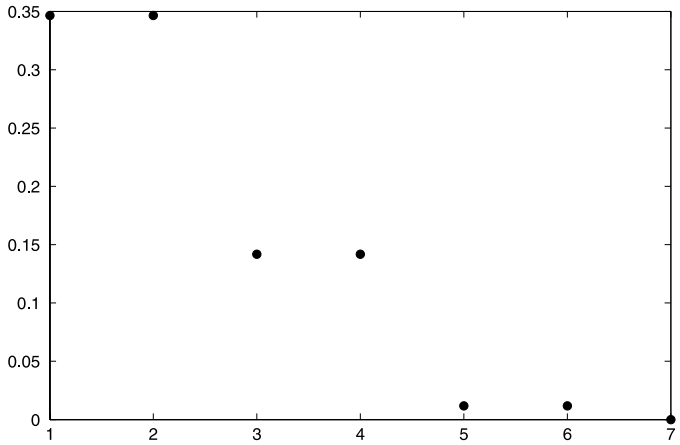

Figure 10. Singular spectrum (normalized) for $N = 7$ particles placed randomly along a figure eight planar curve (i.e. the equilibrium configuration shown in figure 9(*b*)). Singular values are grouped in pairs (except for the zero value) due to the skew-symmetry of the configuration matrix.

Table 1. Singular spectrum of triangular states ($N = 3$).

Configuration	σ (unormalized)	σ (normalized)	Shannon entropy
Equilateral	1.0000	0.5000	0.6931
	1.0000	0.5000	
	0.00	0.00	
Isosceles (acute)	1.0598	0.5000	0.6931
	1.0598	0.5000	
	0.00	0.00	
Isosceles (obtuse)	2.7203	0.5000	0.6931
	2.7203	0.5000	
	0.00	0.00	
Arbitrary triangle	1.2115	0.5000	0.6931
	1.2115	0.5000	
	0.00	0.00	

to our usage here, can be found in http://en.wikipedia.org/wiki/Von_Neumann_entropy. As an example of the normalized spectral distribution associated with the figure eight equilibrium shown in figure 9, we show in figure 10 the 7 singular values (including the zero one) associated with a random placement of points along the figure eight leading to an equilibrium. The fact that they are grouped in pairs follows from the skew-symmetry of A which implies that the eigenvalues come in pairs $\pm\lambda$. Since the singular values are the squares of the eigenvalues, it follows that there are two of each of the non-zero ones.

Tables 1–6 show the complete singular spectrum for all the equilibria considered in this paper. Note that both the shape of the curve and the distribution of points along the curve determine whether this measure of 'entropy' is higher or lower for randomly distributed points versus evenly distributed points for a given curve and value of N. Particularly relevant is the *smallest non-zero singular value* associated with the equilibrium (see, for example, Trefethen and Embree (2005)), as that is a common measure of 'robustness' associated with the configuration matrix, sometimes called the 'spectral gap'. This diagnostic is related to the concept of 'pseudo-spectrum' of A, as described in Trefethen and Embree (2005) and will be further developed in the future to characterize the 'robustness' of the equilibrium.

Table 2. Singular spectrum of collinear states ($N = 3, 7$).

Configuration	σ (unormalized)	σ (normalized)	Shannon entropy
$N = 3$	4.5000	0.5000	0.6931
	4.5000	0.5000	
	0.00	0.00	
$N = 7$ (even)	2.5249	0.3214	1.5237
	2.5249	0.3214	
	1.6831	0.1428	
	1.6831	0.1428	
	0.8420	0.0357	
	0.00	0.00	
$N = 7$ (random)	6.3408	0.4457	1.0723
	6.3408	0.4457	
	2.0969	0.0487	
	2.0969	0.0487	
	0.7062	0.0055	
	0.7062	0.0055	
	0.0000	0.0000	

Table 3. Singular spectrum of circular states ($N = 7$).

Configuration	σ (unormalized)	σ (normalized)	Shannon entropy
$N = 7$ (even)	3.0000	0.3214	1.5236
	3.0000	0.3214	
	2.0000	0.1429	
	2.0000	0.1429	
	1.0000	0.0357	
	1.0000	0.0357	
	0.0000	0.0000	
$N = 7$ (random)	3.7954	0.3363	1.4700
	3.7954	0.3363	
	2.4250	0.1373	
	2.4250	0.1373	
	1.0631	0.0264	
	1.0631	0.0264	
	0.0000	0.0000	

7. Discussion

In this paper we describe a new method for finding and classifying stationary equilibrium distributions of point singularities of source/sink, point vortex, or spiral source/sink type in the complex plane under the dynamical assumption that each point 'goes with the flow'. This dynamical assumption arises in point vortex dynamics through the vorticity 'advection' equation,

$$\vec{\omega}_t + \vec{u} \cdot \nabla \vec{\omega} = 0, \tag{35}$$

where $\vec{\omega}$ is represented by a linear combination of Dirac masses (see Newton (2001)). The corresponding partial differential equation for the source-sink-vortex system that 'goes with the flow' has not been developed and analysed but presumably would not have the Hamiltonian features associated with pure point vortex (i.e. discrete Euler flow) dynamics. We provide examples of configurations placed at random points in the plane, at prescribed points, or lying

Table 4. Singular spectrum of figure eight states ($N = 7$).

Configuration	σ (unormalized)	σ (normalized)	Shannon entropy
$N = 7$ (even)	11.9630	0.4664	0.9651
	11.9630	0.4664	
	3.0001	0.0293	
	3.0001	0.0293	
	1.1454	0.0043	
	1.1454	0.0043	
	0.0000	0.0000	
$N = 7$ (random)	6.9337	0.3465	1.3929
	6.9337	0.3465	
	4.4357	0.1418	
	4.4357	0.1418	
	1.2769	0.0117	
	1.2769	0.0117	
	0.0000	0.0000	

Table 5. Singular spectrum of flower states ($N = 7$).

Configuration	σ (unormalized)	σ (normalized)	Shannon entropy
$N = 7$ (even)	5.9438	0.4447	1.1034
	5.9438	0.4447	
	1.8115	0.0413	
	1.8115	0.0413	
	1.0538	0.0140	
	1.0538	0.0140	
	0.0000	0.0000	
$N = 7$ (random)	8.0780	0.3875	1.3393
	8.0780	0.3875	
	3.8900	0.0899	
	3.8900	0.0899	
	1.9523	0.0226	
	1.9523	0.0226	
	0.0000	0.0000	

along prescribed curves, and find the particle strengths so that the configuration is a stationary equilibrium. This last situation is reminiscent of a classical technique for enforcing boundary conditions along arbitrarily shaped boundaries embedded in fluid flows. These techniques are generically referred to as singularity distribution methods. See, for example, Katz and Plotkin (2001) and Cortez (1996, 2000) for applications and discussions of these methods in the context of potential flow, hence inviscid boundary conditions, and Cortez (2001) in the context of Stokes flow, hence viscous boundary conditions. For these problems, the positions of the points are fixed to lie along the given boundary, and the strengths are then judiciously chosen to enforce the relevant inviscid or viscous boundary conditions. As in Cortez (2001), it would be of interest to 'regularize' the point singularities (1.1) and ask if the methods in this paper can be extended to smoothed out singularities as would a separate analysis associated with the linear and nonlinear stability theory for the stationary equilibria described in this paper about which currently nothing is known. Finally, we mention an interesting paper by O'Neil (2009) which derive several relative equilibria vortex sheets which one can think of as the limit $N \to \infty$ of an N-point vortex problem, with vortex strengths suitably chosen. Whether or not

Table 6. Singular spectrum of spiral states ($N = 7$).

Configuration	σ (unormalized)	σ (normalized)	Shannon entropy
$N = 7$ (even)	6.5969	0.4047	1.2658
	6.5969	0.4047	
	2.9237	0.0795	
	2.9237	0.0795	
	1.3031	0.0158	
	1.3031	0.0158	
	0.0000	0.0000	
$N = 7$ (random)	16.0086	0.4398	1.1024
	16.0086	0.4398	
	5.5884	0.0536	
	5.5884	0.0536	
	1.9593	0.0066	
	1.9593	0.0066	
	0.0000	0.0000	

some of the stationary configurations derived in this manuscript can be extended to the vortex sheet limit so as to maintain the delicate balance that must exist between the global shape of the curve and the choice of singularity strengths is a question we are currently pursuing.

Acknowledgments

This work was supported by The National Science Foundation under Grant NSF-DMS-0804629. We dedicate this work to the memory of Hassan Aref (1950-2011) whose wonderfully elegant work in the field of point vortex dynamics has set a high standard of exposition and clarity for the entire field.

References

Aref H 2009 Stability of relative equilibria of three vortices *Phys. Fluids* **21** 094101
Aref H 2007a Point vortex dynamics: A classical mathematics playground *J. Math. Phys.* **48** 065401
Aref H 2007b Vortices and polynomials *Fluid Dyn. Res.* **39** 5–23
Aref H, Newton P K, Stremler M A, Tokieda T and Vainchtein D L 2003 Vortex crystals *Adv. Appl. Mech.* **39** 1–79
Campbell L J and Kadtke J B 1987 Stationary configurations of point vortices and other logarithmic objects in two dimensions *Phys. Rev. Lett.* **58** 670–3
Cortez R 2000 A vortex/impulse method for immersed boundary motion in high Reynolds number flows *J. Comput. Phys.* **160** 385–400
Cortez R 2001 The method of regularized stokeslets *SIAM J. Sci. Comput.* **23** 1204–25
Cortez R 1996 An impulse based approximation of fluid motion due to boundary forces *J. Comput. Phys.* **123** 341–53
Golub G H and Van Loan C F 1996 *Matrix Computations* 3rd edn (Baltimore, MD: Johns Hopkins Press)
Kadtke J B and Campbell L J 1987 Method for finding stationary states of point vortices *Phys. Rev.* A **36** 4360–70
Katz J and Plotkin A 2001 *Low-Speed Aerodynamics* 2nd edn (Cambridge: Cambridge University Press)
Kochin N E, Kibel' I A and Rose N W 1964 *Theoretical Hydromechanics* 1 (London: Interscience)
Llewellyn Smith S G 2011 How do singularities move in potential flow? *Physica* D **240** 1644–51
Newton P K 2001 *The N-Vortex Problem: Analytical Techniques* (New York: Springer)
Newton P K and Chamoun G 2009 Vortex lattice theory: A particle interaction perspective *SIAM Rev.* **51** 501–42
Novikov E A 2003 Dynamics of distributed sources *Phys. Fluids* **15** L65–7
Novikov A E and Novikov E A 1996 Vortex-sink dynamics *Phys. Rev.* E **54** 3681–6
Novikov E A and Sedov Yu B 1983 Concentration of vorticity and helical vortices *Fluid Dyn.* **18** 6–12

Shannon C E 1948 A mathematical theory of communication *Bell Syst. Tech. J.* **27** 379–423
O'Neil K A 1987 Stationary configurations of point vortices *Trans. AMS* **302** 383–425
O'Neil K A 2009 Relative equilibria of vortex sheets *Physica* D **238** 379–83
Trefethen L N and Bau D III 1997 *Numerical Linear Algebra* (Philadelphia: SIAM)
Trefethen L N and Embree M 2005 *Spectra and Pseudospectra: The Behavior of Nonnormal Matrices and Operators* (Princeton: Princeton University Press)
Tur A, Yanovsky V and Kulik K 2011 Vortex structures with complex point singularities in two-dimensional Euler equations. New exact solutions *Physica* D **240** 1069–79
Yanovsky V V, Tur A and Kulik K N 2009 Singularities motion equations in 2-dimensional ideal hydrodynamics of incompressible fluid *Phys. Lett.* A **373** 2484–7